



## Full Length Article

# A possible role of tachykinin-related peptide on an immune system activity of mealworm beetle, *Tenebrio molitor* L.

A. Urbański<sup>a,b,\*</sup>, N. Konopińska<sup>a</sup>, J. Lubawy<sup>a</sup>, K. Walkowiak-Nowicka<sup>a</sup>, P. Marciniak<sup>a</sup>, J. Rolff<sup>c,d</sup>

<sup>a</sup> Department of Animal Physiology and Developmental Biology, Adam Mickiewicz University, Uniwersytetu Poznańskiego Str. 6, 61-614, Poznań, Poland

<sup>b</sup> HiProMine S.A, Poznańska Str. 8, 62-023, Robakowo, Poland

<sup>c</sup> Evolutionary Biology, Institute for Biology, Freie Universität Berlin, Königin-Luise-Str. 1-3, 14195, Berlin, Germany

<sup>d</sup> Berlin-Brandenburg Institute of Advanced Biodiversity Research (BBIB), Königin-Luise-Str. 2-4, 14195, Berlin, Germany



## ARTICLE INFO

## Keywords:

Tachykinins  
Neuropeptides  
Insect haemocytes  
Cellular response  
Phenoloxidase

## ABSTRACT

Tachykinin-related peptides (TRPs) are important neuropeptides. Here we show that they affect the insect immune system, especially the cellular response. We also identify and predict the sequence and structure of the tachykinin-related peptide receptor (TRPR) and confirm the presence of expression of gene encoding TRPR in *Tenebrio molitor* haemocytes.

After application of the Tenmo-TRP-7 in *T. molitor* the number of circulating haemocytes increased and the number of haemocytes participating in phagocytosis of latex beads decreased in a dose- and time-dependent fashion. Also, Tenmo-TRP-7 affects the adhesion ability of haemocytes. Six hours after injection of Tenmo-TRP-7, a decrease of haemocyte surface area was observed under both tested Tenmo-TRP-7 concentrations ( $10^{-7}$  and  $10^{-5}$  M). The opposite effect was reported 24 h after injection, which indicates that the influence of Tenmo-TRP-7 on modulation of haemocyte behaviour differs at different stages of stress response. Tenmo-TRP-7 application also resulted in increased phenoloxidase activity 6 and 24 h after injection.

The assessment of DNA integrity of haemocytes showed that the injection of Tenmo-TRP-7 at  $10^{-7}$  M led to a decrease in DNA damage compared to control individuals. This effect was only visible 6 h after Tenmo-TRP-7 application. After 24 h, Tenmo-TRP-7 injection increased DNA damage.

We also confirmed the expression of immune-related genes in nervous tissue of *T. molitor*. Transcripts for genes encoding receptors participating in pathogen recognition processes and antimicrobial peptides were detected in *T. molitor* brain, retrocerebral complex and ventral nerve cord. These results may indicate a role of the insect nervous system in pathogen recognition and modulation of immune response similar to vertebrates.

Taken together, our results support the notion that tachykinin-related peptides probably play an important role in the regulation of the insect immune system. Moreover, some resemblances with action of tachykinin-related peptides and substance P showed that insects can be potential model organisms for analysis of hormonal regulation of conserved innate immune mechanisms.

## 1. Introduction

During a stress response many insect physiological systems cooperate to return to homeostasis (Adamo, 2014). Due to high energy cost associated with maintaining and employing the immune system, a fine-tuned balance between activity and the usage of available resources is required (Adamo, 2017). Recent research clearly showed that, similar to vertebrates, in insects stress responses are regulated by hormones,

especially octopamine (OCT), a structural and functional homologue of norepinephrine, and adipokinetic hormones (AKHs) which in insects play a role similar to glucagon in mammals (Adamo, 2014; Chowanski et al., 2017). Both compounds regulate insect metabolism and immune system activity, and very often cause similar effects.

The mechanisms of interactions between the endocrine and the immune system in insects still remain largely unknown. Based on the knowledge about hormonal regulation during stress responses in

\* Corresponding author. Department of Animal Physiology and Developmental Biology, Adam Mickiewicz University, Uniwersytetu Poznańskiego Str. 6, 61-614, Poznań, Poland.

E-mail address: [arur@amu.edu.pl](mailto:arur@amu.edu.pl) (A. Urbański).

<https://doi.org/10.1016/j.dci.2021.104065>

Received 6 January 2021; Received in revised form 19 February 2021; Accepted 2 March 2021

Available online 8 March 2021

0145-305X/© 2021 The Author(s). Published by Elsevier Ltd. This is an open access article under the CC BY license (<http://creativecommons.org/licenses/by/4.0/>).

vertebrates, we can assume that not only these two hormones participate in regulation of insect immune system functioning during stress response. Current knowledge about structural and functional homology between insect and vertebrate endocrine systems and the existence of similar dependencies between stress hormones suggests that the missing element in this puzzle could be tachykinin-related peptides (TRPs), structural and functional homologues of tachykinins (TKs) (Urbański and Rosiński, 2018).

Tachykinin-related peptides are one of the largest families of neuropeptides (Nässel et al., 1999). The high level of structural homology of TRPs and TKs was confirmed by Li et al. (1991) and Nachman et al. (1999). These authors confirmed that substance P (SP, one of the mammalian tachykinins) can activate the TRP receptor. The SP antagonist spantide 1, is a potent antagonist of invertebrate TRPs (Nässel, 1999). This is explained by the similarity in conformation of these neuropeptides, and also the sequence at the C-terminal end (invertebrate - FXGXRA; vertebrate - FXGLMa) and its amidation, which is crucial for the elicitation of physiological effects (Li et al., 1991; Nachman et al., 1999; Nässel, 1999).

Close evolutionary relationships between TRPs and TKs are also mirrored in their functions: they contribute to the regulation of nociception and muscle contractions (Chowanski et al., 2017; Nässel et al., 1999). Moreover, similar to SP, TRPs possess antimicrobial properties (Diniz et al., 2020). However, some important properties of TKs have not been described for insect TRPs, especially their role in regulation of immune system activity. Studies about SP showed that this neuropeptide plays an important role in the immune system including stimulation of immune-related cells and the modulation of humoral responses by cytokine release (O'Connor et al., 2004). For this reason, we proposed that insect TRPs can influence cellular and humoral immune mechanisms (Urbański and Rosiński, 2018). The evaluation of this hypothesis is the main aim of the present study. The physiological analysis is combined with the prediction of the structure of a TRP receptor of *T. molitor* (Tenmo-TRPR) and a study of the presence of this receptor on haemocyte surfaces to investigate whether TRPs act directly or indirectly on haemocytes. In addition, to support a close relationship between insect nervous tissues and the immune system, the expression of pattern recognition receptors (PRRs) and main elements of basic immune-related pathways in the *T. molitor* nervous system was investigated.

## 2. Materials and Methods

### 2.1. Insects and haemolymph collection

Only 7-day-old adult males of *T. molitor* were used. Beetles were cultured at the Institute of Zoology, Freie Universität Berlin and at the Department of Animal Physiology and Developmental Biology, Adam Mickiewicz University according to a method previously described by El-Shazely et al. (2019). Adult males were kept in the dark, at 28 °C. To avoid potential infection and contact between tested individuals, beetles were kept in sterile, compartmentalized square plastic dishes.

Before neuropeptide injection or haemolymph collection, beetles were anesthetized with CO<sub>2</sub>. Neuropeptide was injected under the coxa of the third pair of legs. Haemolymph was collected by cutting the tibia of the first pair of legs, which ensures obtaining a sample of haemolymph without contaminations.

### 2.2. Peptides

The neuropeptide Tenmo-TRP-7 (MPRQSGFFGMRA) was used for all experiments, because of its structural similarity to SP (RPKPQQFFGLMa) (Fig. S1). The neuropeptide was synthesized by Creative Peptides (Shirley, NY, USA; purity >95% HPLC). 2 µL of neuropeptide solution in physiological saline was injected 6 or 24 h before analysis in concentrations of 10<sup>-7</sup> and 10<sup>-5</sup> M (final concentration in

insects 10<sup>-8</sup> and 10<sup>-6</sup> M, respectively). The total haemolymph volume of *T. molitor* is about 20 µL (Marciniak et al., 2017). The concentrations were based on previous studies of neuropeptides in insects and research on the influence of SP on immune cells (Hernández-Martínez et al., 2017; Marciniak et al., 2020; Mashaghi et al., 2016; Monaco-Shawver et al., 2011).

### 2.3. Transcriptome sequencing, database search and sequence comparison

Transcriptomic data from *T. molitor* [BioProject: PRJNA608239; Sequence Read Archives (SRA): SRR11184806] from the brain and retrocerebral complex of adult beetles obtained by Marciniak et al. (2020) were reanalyzed and used for database search and sequence comparison by local tblastn. For local tblastn, a sequence of *Tribolium castaneum* TRPR (XP\_008194527.2) was used to identify a sequence of *T. molitor* TRPR.

For the analysis of putative transmembrane regions in the predicted protein sequence of the Tenmo-TRPR ORF (open reading frame) PSIPRED—MEMSAT software (<https://bioinf.cs.ucl.ac.uk/psipred/>) was used (Nugent and Jones, 2009). Prediction of glycosylation, palmitoylation and phosphorylation was performed using, respectively, NetNGlyc 1.0, CSS-PALM 4.0 and NetPhos 3.1 (<https://www.cbs.dtu.dk/services/NetNGlyc/>, <https://csspalm.biocuckoo.org/online.php>, <https://www.cbs.dtu.dk/services/NetPhos/>) (Blom et al., 2004; Ren et al., 2008). In addition, a two-dimensional representation of the receptor was created in TOPO2 (Johns S.J., TOPO2, transmembrane protein display software, <https://www.sacs.ucsf.edu/TOPO2/>).

Protein sequence alignment of Tenmo-TRPR with other Coleopteran TRPRs was performed with Clustal W (<https://embnet.vital-it.ch/software/ClustalW.html>) and includes *T. castaneum* (XP\_008194527.2), *Aethina tumida* (XP\_019866300.1), *Nicrophorus vespilloides* (XP\_017769025.1) and *Rhynchophorus ferrugineus* (QGA72520.1). To compare Tenmo-TRPR sequence with other insect species and human neurokinin receptors (NKR) the following sequences were used: NP\_524556.2 for *D. melanogaster*; XP\_001652376.3 for *Aedes aegypti*, AAA59936.1, AAB05897.1 and AAB21706.1 for human NK1R, NK2R and NK3R, respectively. All alignments and similarity analysis were visualized with usage of Jalview and Ugene software.

### 2.4. Presence of gene encoding TRP receptor in haemocytes

Transcript profiles of the gene encoding Tenmo-TRPR were determined by reverse transcriptase PCR (RT-PCR) in selected tissues of *T. molitor* males. RT-PCR was performed according to a modification of the method described by Marciniak et al. (2020). Suitable tissues (brain, ventral nerve cord and haemocytes) were transferred to 150 µL of RNA lysis buffer (Zymo Research, USA) and homogenized for 3 min using a pellet homogenizer (Kimble Chase, USA). The homogenized tissues were immediately frozen in liquid nitrogen and then stored at -80 °C. For RNA isolation A Quick-RNA® Mini Prep kit (Zymo Research, USA) was used. Quantification and verification of isolated RNA was performed using the Synergy H1 Hybrid Multi-Mode Microplate Reader (BioTek, USA). Reverse transcription of the same amount of isolated RNA (200 ng) to cDNA was accomplished using the RevertAid™ Reverse Transcriptase kit (Thermo-Fisher Scientific, USA) according to the manufacturer's protocol. RT-PCR analyses were conducted using a T100™ Thermal Cycler (Bio-Rad, USA). The primers were designed based on sequences of Tenmo-TRPR using Primer3 software (Untergasser et al., 2012). The primer pair was created to amplify fragments of 177 bp with the following sequences Fw 5'- TTATCCAGAATGGCCGACG -3' and Rev 5'- CATTTGCCTCTGCGTGCATT -3'. The primers were synthesized by the Institute of Biochemistry and Biophysics of the Polish Academy of Science (Warsaw, Poland). RT-PCR was performed in a 10 µL reaction volume containing: 3.95 µL of DNase/RNase-free water, 1 µL of Dream-Taq™ Green Buffer (Thermo-Fisher Scientific, USA), 1 µL of 2 mM dNTP,

1  $\mu\text{L}$  of 10  $\mu\text{M}$  forward primers, 1  $\mu\text{L}$  of 10  $\mu\text{M}$  reverse primers, 0.05  $\mu\text{L}$  of DreamTaq™ DNA polymerase (Thermo-Fisher Scientific, USA) and 2  $\mu\text{L}$  of cDNA. The obtained products were analysed by electrophoresis using a 2% TAE agarose gel stained with ethidium bromide. The Quick-Load Purple 100 bp DNA Ladder (New England BioLabs, USA) was run on each gel. Photos of the agarose gels were taken using ChemiDoc™ Touch (Bio-Rad, USA). Minimum of 5 biological and 2 technical repeats were made. To confirm our results, the bands were sequenced with BigDye Terminator v3.1 on an ABI Prism 3130XL Analyzer (Applied Biosystems, Foster City, CA, USA) according to manufacturer's protocols by the Laboratory of Molecular Biology Techniques (Faculty of Biology, Adam Mickiewicz University in Poznań) and compared with transcriptomic data. For checking potential foreign DNA or genomic DNA contamination of samples, "No template control" (DNA/RNA free water) and "no RT control" reactions were included in the analysis (Fig. S2).

## 2.5. Total haemocytes count

The number of circulating haemocytes was determined following Urbański et al. (2018). In this assay, 2  $\mu\text{L}$  of haemolymph were mixed with 20  $\mu\text{L}$  of physiological saline (PS) appropriate for beetles (274 mM NaCl, 19 mM KCl, 9 mM CaCl<sub>2</sub>) and an anticoagulation buffer (4.5 mM citric acid and 9 mM sodium citrate, 5:1 v/v). The total haemocyte count (THC) was then determined using a Bürker chamber and a Zeiss PrimoStar light microscope equipped with an Axiocam 105 digital camera. In each replicate, 24 randomly selected fields of the Bürker chamber were analysed and counted using ImageJ (version 2) software. At least 10 individuals were used in each of the treatments and three independent replications were conducted.

## 2.6. Phagocytic ratio

The ability of haemocytes to phagocytose latex beads (Sigma-Aldrich L1030) was assessed as described in Urbański et al. (2014). We also determined the direct influence of neuropeptides on haemocytes by adding Tenmo-TRP-7 to physiological saline, during incubation of haemocytes with latex beads (*in vitro* experiment). The final concentration of neuropeptides in the suspension was  $10^{-8}$  and  $10^{-6}$  M respectively, which corresponds to neuropeptide concentrations of  $10^{-7}$  and  $10^{-5}$  M in the insect body after injection. Haemolymph samples were incubated on a microscopic slide coated with poly-L-lysine for 30 min at room temperature, together with a suspension of latex beads (Sigma-Aldrich L1030) and physiological saline with an anticoagulation buffer (600:1 v/v). Excess suspension was removed and the sample was washed with physiological saline. After washing, the haemocytes were fixed with a 4% paraformaldehyde solution for 10 min. Next, the samples were mounted with mounting medium (glycerol for fluorescent microscopy, Sigma Aldrich 1.04095) and analysed with a Nikon Eclipse Ti2 microscope equipped with Nikon DS-Qi2 digital camera. For a better recognition of phagocytosis, cellular responses were confirmed with light microscopy. Five images for each sample were taken. Photos were analysed with ImageJ (version 2) software, and the results were expressed as the mean percentage of cells with fully phagocytosed beads of the total number of haemocytes on the images. For the minimization of error related to the individual variance between beetles, samples were compared to the control samples performed always in the same day as the groups treated by Tenmo-TRP-7. For estimation of phagocytic ratio at least 3260 haemocytes from 9 individuals were counted.

## 2.7. Haemocyte morphology and surface area

Haemocyte morphology was analysed based on the method described by Czarniewska et al. (2012) that focuses on the arrangement of the F-actin cytoskeleton. After neuropeptide injection, haemolymph samples were mixed with, as described previously, a solution of physiological saline and an anticoagulation buffer (5:1 v/v). Direct effect of

tested compounds on haemocytes morphology was determined by incubation of haemolymph samples with solution of physiological saline, anticoagulation buffer and neuropeptides in concentrations corresponding to final neuropeptide concentrations in the insect body ( $10^{-8}$  M and  $10^{-6}$  M). Samples were incubated on a microscope slide coated with poly-L-lysine (Sigma-Aldrich P4707) for 30 min at room temperature. After incubation, the samples were washed, fixed with a 4% solution of paraformaldehyde in physiological saline and permeabilized with 0.1% Triton-X 100 (Sigma-Aldrich T8532). Then, the haemocyte F-actin cytoskeleton was stained with Oregon Green® 488 phalloidin (Invitrogen) for 25 min in the dark at room temperature. To visualize nuclear DNA, a solution of DAPI in physiological saline (1:50 v/v) was used. After staining, the samples with mounting medium (90% glycerol with 2.5% DABCO) were mounted. Haemocytes were analysed with a Nikon Eclipse TE 2000-U fluorescence microscope. The photos were taken using a Nikon DS-1QM camera.

Based on the obtained micrographs, the surface area of *T. molitor* haemocytes was determined using AxioVision software (ver. 4.8.2.). To minimize the individual variation between insects, treatment groups were compared to the control samples performed on the same day. To quantify changes observable under the microscope, at least 220 haemocytes from 7 individuals were measured. The assay was repeated at least three times.

## 2.8. Comet assay - assessment of DNA integrity of haemocytes

Haemocyte DNA integrity was measured following Lubawy et al. (2019). To avoid any UV-related DNA damage of isolated cells, all the following steps were performed under dimmed light. After anaesthesia, the right, front leg was cut off at the tibia and 2  $\mu\text{L}$  of haemolymph was collected into 20  $\mu\text{L}$  of physiological saline containing an anticoagulation buffer (5:1 v/v). Next the cells were combined in a 1.5 mL tube filled with molten LMAgarose in 1:10 (v:v) ratio and immediately pipetted onto microscope slides. After gelling of the agarose, the slides were placed in a pre-chilled Lysis solution for 60 min. Next the slides were immersed for 30 min in alkaline solution (300 mM NaOH, 1 mM EDTA, pH > 13) and then washed twice in 1xTBE buffer (80 mM Tris Base, 89 mM boric acid, 3.2 mM EDTA) for 2 min. Slides were then placed flat onto a gel tray and aligned equidistant from the electrodes. The voltage was set to 1 V per cm (measured electrode to electrode) and applied for 10 min. After electrophoresis samples were dipped in 70% ethanol for 5 min and dried in an incubator set to 37 °C. Comets were stained with 10x CYGREEN® Dye for 30 min and visualized using a Nikon Eclipse TE 2000-U fluorescence microscope equipped with a Nikon DS-1QM camera (Nikon, Tokyo, Japan). In order to provide a positive control for each step in the comet assay, one slide with cells that had been treated with H<sub>2</sub>O<sub>2</sub> was prepared for every electrophoretic run. The cells, which were isolated from randomly selected control animals, were treated with H<sub>2</sub>O<sub>2</sub> (100  $\mu\text{M}$ , Sigma-Aldrich, St. Louis, USA) for 10 min, and after which they were tested for DNA damage under the same conditions as described above. For each treatment, 5–6 different treated animals were used, each produced one slide of haemocytes to analyze. At least 50 nuclei from 10 randomly captured images were analysed per slide (i.e. 10 images/slide and 5–6 slides/treatment). Assessment of DNA integrity of haemocytes was determined using OpenComet software according to the method described by Gyori et al. (2014). DNA integrity was evaluated based on the three parameters: tail moment (tail length x % of DNA in the tail), % of DNA in the tail and % of DNA in the head.

## 2.9. Phenoloxidase activity

Phenoloxidase was assayed as previously described by Sorrentino et al. (2002) and Urbański et al. (2018). Haemolymph samples (1  $\mu\text{L}$ ) were placed on white filter paper soaked with DL-DOPA (2 mg/1 mL) in a 10 mM phosphate buffer and incubated for 30 min at room temperature in the dark. For each of the tested individuals two technical replicates

were analysed. After incubation, the filter papers were air-dried, scanned by SHARP AR 153 EN (600 dpi, 8 bits, grayscale), and analysed with ImageJ (version 2) software. Results are expressed as mean pixel value measured for the centre part of each sample (40 pixels). At least 10 individuals were used in each treatment.

## 2.10. Presence of immune-related genes in nervous tissues

The possible presence of immune-related genes in selected nervous tissue of *T. molitor* was analysed based on previously mentioned transcriptomic data from the brain and retrocerebral complex of adult beetles. Moreover, this analysis was confirmed by RT-PCR analysis of expression of genes encoding selected immune-related receptors and antimicrobial peptides. The receptors and AMPs sequences used for local blastn were mainly based on the sequences previously published by Jacobs et al. (2017) and Johnston et al. (2014).

RT-PCR analyses were performed according to the method described above. The primers for immune-related genes were synthesized according to sequence used before by Jacobs et al. (2017). Only primers for *domeless* were designed based on available data (NCBI Reference Sequence: XM\_001807008.3) using Primer3 software (Untergasser et al., 2012) (Table S1, list of used primers). The transcript profiles of immune-related genes were determined in the brain, ventral nerve cord (VNC), retrocerebral complex and, as reference, in fat body and haemocytes of *T. molitor* adults.

## 2.11. Statistical analysis

For the statistical analysis GraphPad Prism 5 software was used (Adam Mickiewicz University license). The normality of the distribution in each tested research variant was determined with the Shapiro-Wilk test. For checking of homogeneity of variance Brown-Forsythe test and the Levene test were used. Normally distributed data were analysed with the Student's *t*-test with Welch's correction. Non-normally distributed data were analysed with the Kruskal-Wallis test and the Mann-Whitney *U* test.

## 3. Results

### 3.1. Analysis of *T. molitor* TRPR sequence

Based on the BLAST search using the local database the transcriptomic assembly of *T. molitor* brain and retrocerebral complex yielded an open reading frame with 1287 bp which encodes a putative tachykinin-related peptide receptor (Fig. 1).

The Tenmo-TRPR displays the seven transmembrane domains typical for GPCRs (G-protein coupled receptors) (Bass et al., 2014) with *N*-terminal ligand binding tail and *C*-terminal intracellular region (Fig. 2). The predicted post translational modifications of the receptor protein include the typical glycosylation of *N*-terminal region and extracellular loops, phosphorylation by protein kinase C and cAMP and cGMP dependent kinases and palmitoylation at the *C*-terminal tail (Fig. 2).

Protein sequence alignment with other beetles showed a high degree (>67%) of identity (Fig. S3). The highest identity was observed with *T. castaneum* (93%) from the family Tenebrionidae, the lowest with

*N. vespilloides* (68%). Also, comparison of Tenmo-TRPR sequence to Dipteran model species showed a high level of identity (62% for *D. melanogaster* and 71% *Ae. aegypti*). Tenmo-TRPR compared to human neurokinin receptors, showed identities of 43% to human NK3R, 41% to human NK1R and 37% to human NK2R (Fig. S4).

### 3.2. Presence of the gene encoding the TRP receptor in haemocytes

The results of RT-PCR analysis indicated the expression of the gene encoding Tenmo-TRPR in haemocytes which may suggest the presence of this receptor on the haemocyte surface (Fig. 3).

### 3.3. Total haemocytes count

The influence of Tenmo-TRP-7 on the number of circulating haemocytes was time-dependent (Fig. 4). The application of  $10^{-5}$  M Tenmo-TRP-7 led to a significant increase in THC 24 h after injection (Welch *t*-test,  $t = 2.39$ ;  $p \leq 0.05$ ). It should be mentioned that, despite a lower average number of haemocytes in control beetles 24 h after PS injection than in control beetles 6 h after PS injection, differences between both control groups were not observed.

### 3.4. Phagocytic ratio

The number of phagocytically active haemocytes was reduced after application of Tenmo-TRP-7 in the highest concentration ( $10^{-6}$  M) in *in vitro* conditions only (Mann-Whitney *U* test,  $U = 9.00$ ;  $p \leq 0.05$ ) (Fig. 5).

### 3.5. Haemocytes morphology and their surface area

Tenmo-TRP-7 did not influence the arrangement of F-actin cytoskeleton of *T. molitor* haemocytes in all treatments (Fig. 6 and S5). Only haemocyte size differed which may indicate different adhesion ability and time of haemocytes sedimentation. These observations were confirmed by analysis of changes of haemocytes surface area (Fig. 7). In this case, the effect of Tenmo-TRP-7 was time-dependent. However, no significant differences were observed in case of direct effect of tested neuropeptide on *Tenebrio* haemocytes (Fig. 7 and S3). After 6 h individuals injected with Tenmo-TRP-7 ( $10^{-7}$  and  $10^{-5}$  M) displayed a significant decrease of haemocyte surface area compared to controls (Kruskal-Wallis test,  $H = 6.91$ ,  $p \leq 0.05$ ). By contrast, 24 h after injection of Tenmo-TRP-7 in  $10^{-5}$  M a significant increase in haemocyte surface area was observed (Mann-Whitney *U* test,  $U = 1145.00$ ;  $p \leq 0.05$ ) (Figs. 6 and 7).

### 3.6. DNA damage

The effects of Tenmo-TRP-7 application were time-dependent (Fig. 8 and Fig. S6). Six hours after injection of Tenmo-TRP-7 at a concentration of  $10^{-7}$  M a decrease in DNA damage was observed, as indicated by significant decrease in tail moment (Mann-Whitney *U* test,  $U = 126938.00$ ;  $p \leq 0.05$ ) (Fig. 8A) and tail DNA % (Mann-Whitney *U* test,  $U = 130107.00$ ;  $p \leq 0.01$ ) (Fig. 8B) and increasing the percentage of head DNA (Mann-Whitney *U* test,  $U = 130107.00$ ;  $p \leq 0.01$ ) (Fig. 8C). By contrast, 6 h after application of Tenmo TRP-7 at a concentration  $10^{-5}$  M, an increase was found (Mann-Whitney *U* test; tail DNA % -  $U =$

```

7m TRPR      1  MNSTQEFLLYTTNRSYLDNSSLFEGIPINGTGNDEQDGNQFILPVVQRQLWLSILYAQMVLVATGGNLLIVIVLVSQHKRMRVTVTVYFLLNLSVADTMVSTLNVTFNFVYMLNSHWPFGE 118
7m TRPR      119  LYKIKISQFIAVLVSCASVFLMSISDRYMAIMTPLRPRMGRVTYLLAVSTWLLGIIIGSPSLMFFRRTYTMPYKDGEEERVICYPEWPDGSTNESMMEVLYNVGFLFVTVVVPVIGSMT 236
7m TRPR      237  FTYARIGIEIWLWGSQSIGECTQRQEMENIRSKRRVVKMMVVVVIIFAVCWLPYHLYFIVISYFPEITSSTYIQETYLAIYWLAMSNMYPNPIIYCNMNAARFRRGFKQFFSCLPFIHVSPO 354
7m TRPR      355  ALTRREVLTSRRRSYSGSPDHNRIIRNGTIRMNYITRPSPTSSTNTCYSNLFPDETAYHRGQEPRRWKGDRLRSVS

```

Fig. 1. Tenmo-TRPR amino acid sequence. Transmembrane helices are highlighted with boxes.

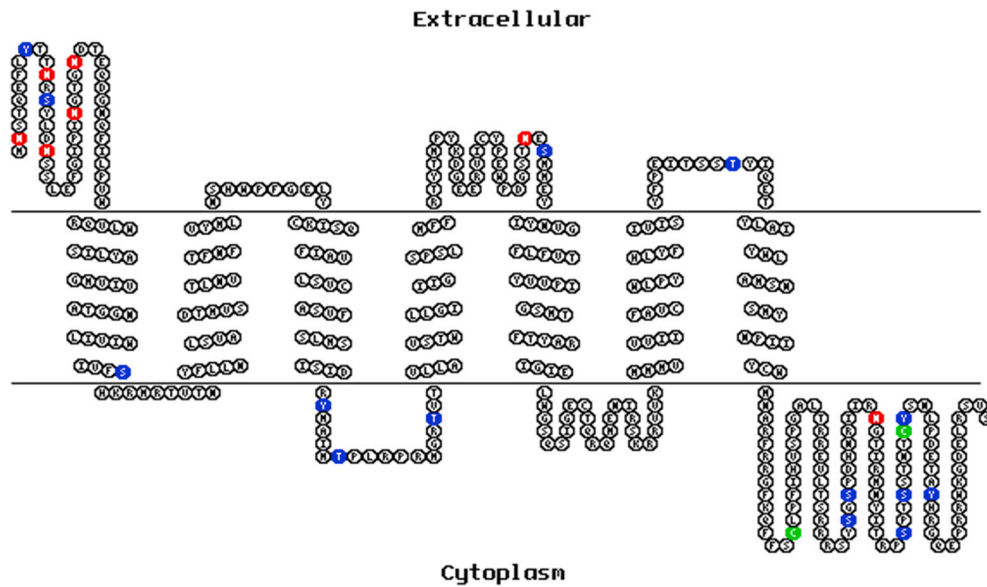


**Fig. 2.** Protein structure model of *T. molitor* TRPR. The schematic representations indicate the orientation of the receptor protein and seven transmembrane domains. Predicted glycosylation sites are highlighted in red, in blue putative phosphorylation sites and in green predicted palmitoylation sites.

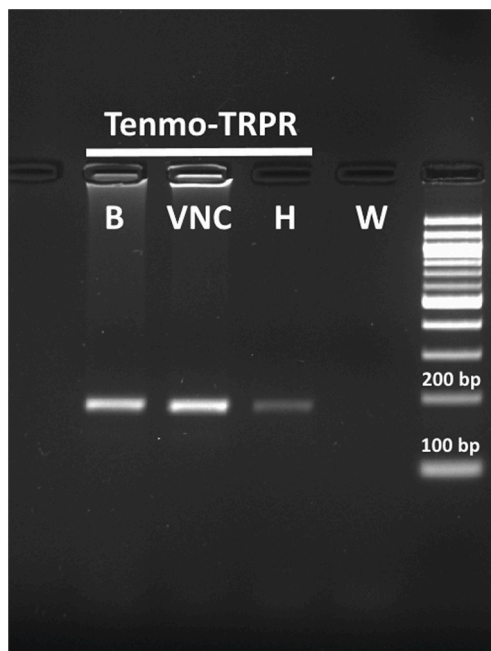


**Fig. 3.** Expression of gene encoding tachykinin-related peptides receptor (Tenmo-TRPR) in different tissues of *Tenebrio molitor*; B – brain; VNC – ventral nerve cord; H – haemocytes; W – water.

91972.000;  $p \leq 0.001$ ; head DNA % -  $U = 91973.000$ ;  $p \leq 0.001$ ) (Fig. 8B and C). 24 h after application of TRP-7 in concentration  $10^{-7}$  M shows an increase of DNA damage. In this group, compared to control, the tail moment and tail DNA % significantly increased (Mann-Whitney  $U$  test,  $U = 158259.00$ ;  $p \leq 0.01$ ; Kolmogorov-Smirnov test,  $D = 0.10$ ;  $p \leq 0.05$ , respectively) (Fig. 8A and B). Moreover, head DNA % decreased significantly (Kolmogorov-Smirnov test,  $D = 0.10$ ;  $p \leq 0.05$ ) (Fig. 8C). In case of application of tested neuropeptide in concentration  $10^{-5}$  M no significant changes were noted. The biggest changes were observed in the group treated with  $H_2O_2$  (the positive control for the Comet assay) (Fig. 8).

### 3.7. Phenoloxidase activity

The influence of Tenmo-TRP-7 in both tested concentrations was similar: after 6 and 24 h after injection an increase in PO activity in *T. molitor* haemolymph was observed (Fig. 9). This was significant in both tested concentrations at 6 h (Welch's  $t$ -test;  $t = 3.55$ ,  $p \leq 0.05$  and  $t = 2.73$ ,  $p \leq 0.05$ , respectively for  $10^{-7}$  and  $10^{-5}$  M), but after 24 h only for the lower concentration of Tenmo-TRP-7 (Mann-Whitney  $U$  test,  $U = 20.00$ ,  $p \leq 0.05$ ).

### 3.8. Presence of immune-related gene expression in nervous tissues

Bioinformatic analysis of a transcriptome of the *T. molitor* brain and the retrocerebral complex showed that the transcripts characteristic for immune-related genes are present in these structures, including genes encoding main components of canonical immune pathways (Toll, Imd, JAK-STAT) and antimicrobial peptides (AMPs) (Table S2). Moreover, transcripts for other receptors participating in regulation of immune system functioning, such as a Scavenger or Nimrod, were also found. The expression of almost each of the putative genes encoding AMPs were reported. Only transcripts for Thaumatin 1 and 2 (only in case of brain) and Defensin 2 (only in case of CC/CA) and 3 were not found. To verify the transcriptomic analysis, expression of genes encoding chosen receptors and AMPs using RT-PCR were analysed (Figs. 10 and 11). In each of the cases, RT-PCR confirmed the expression of immune-related genes in the brain, the retrocerebral complex and also in the VNC. In the case of Thaumatin, two products were obtained (Fig. 11.). However, in both cases, sequencing results indicate a different form of Thaumatin.

## 4. Discussion

The knowledge about neurohormonal regulation of the insect immune system is still in its infancy. The main aim of the presented research was the analysis of the influence of TRP on the immune defence of *T. molitor*, especially on the cellular response. This was motivated by the physiological actions of tachykinins, the functional and structural homologues of insect TRPs. For this reason, one of the most important questions was whether TRP can directly influence *T. molitor* haemocytes and shape their behaviour? The results of RT-PCR assay confirmed the presence of transcript for Tenmo-TRPR gene on *T. molitor* haemocytes, which may suggest the presence of the receptors on the surface of these

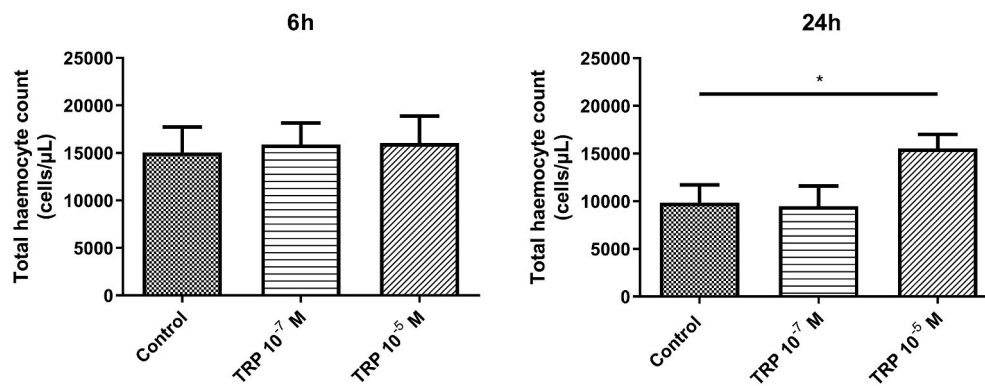


Fig. 4. Total haemocyte count in *Tenebrio molitor* haemolymph after injection of Tenmo-TRP-7 in concentration  $10^{-7}$  and  $10^{-5}$  M; 6 and 24 h after injection. Control – individuals injected with physiological saline appropriate for beetles. Values are means  $\pm$  SEM. \* $p \leq 0.05$  ( $n \geq 10$ ).

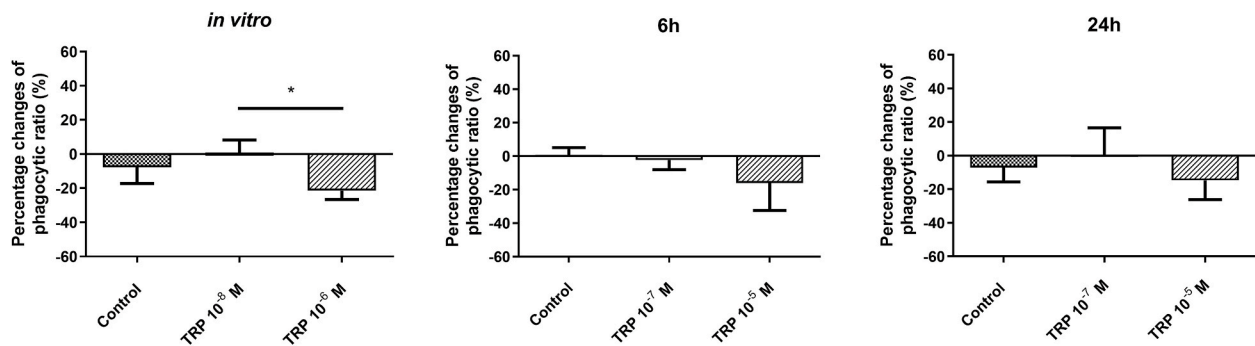


Fig. 5. Percentage changes of phagocytic ratio of *Tenebrio molitor* haemocytes. *in vitro* – direct effect of Tenmo-TRP-7 on haemocytes from untreated donors in concentration corresponding to neuropeptides concentration in insect body after injection  $10^{-7}$  M and  $10^{-5}$  M dilution (final concentration  $10^{-8}$  M and  $10^{-6}$  M). 6 h and 24 h – haemocytes collected 6 or 24 h after injection of Tenmo-TRP-7 in concentration  $10^{-7}$  M and  $10^{-5}$  M. The results are expressed as a percentage change compared to control individuals injected with physiological saline or non-injected beetles (*in vitro*). Values are means  $\pm$  SEM. \* $p \leq 0.05$  ( $n \geq 9$ ).

cells. This result is expected because receptors for stress hormones, e.g. for AKH, have been previously identified on the haemocyte surface (Ziegler et al., 2011). Moreover, neurokinin receptors (vertebrate receptors for tachykinins) are present on vertebrate immune-related cells, like macrophages (Ho et al., 1997). Also, the research conducted by Nagai-Okatani et al. (2016) on *Bombyx mori* partially support this assumption, because the transcript for gene encoding TRP was also present in silkworm haemocytes.

The transcriptomic data also allows us to predict the sequence and structure of Tenmo-TRP. The first evidence of presence of receptor for TRP in insects was shown by Li et al., in 1991. These authors, using the probes from the bovine substance K receptor (one of the neurokinin receptors), found it in the *D. melanogaster* embryo. Until now, the presence of TRPR were shown in different tissues of many insect species, including another representative of Tenebrionidae, the model species *T. castaneum* (Hauser et al., 2008). The predicted sequence of Tenmo-TRPR displays the seven transmembrane domains typical for GPCRs and TRPR and showed a high level of identity compared to other Coleopteran species (no less than 65%). Similar to other insect TRPRs, also Tenmo-TRPR shows quite high degree of identity to vertebrate neurokinin receptors, including human neurokinin receptor NK1R, NK2R and NK3R (about 37–43%) (Van Loy et al., 2010). Due to this identity Tenmo-TRPR can be classified into the large family of neurokinin receptors (or tachykinin receptors), members of the class A family of seven-transmembrane GPCRs.

Based on these findings, the direct *in vitro* and *in vivo* (injection) effects of Tenmo-TRP-7 application on the cellular response were analysed. The effect of Tenmo-TRP-7 application on *T. molitor* haemocytes in many cases was dose- and time-dependent. In case of THC value, the number of circulating haemocytes did not change 6 h after application of

Tenmo-TRP-7 in different concentrations but after 24 h the higher concentration ( $10^{-5}$  M) led to a significant increase in the number of haemocytes. Generally during stress responses an increase in the number of circulating haemocytes is observed (Adamo, 2010; Mowlds et al., 2008). Moreover, research by Adamo (2010) showed that application of octopamine, one of the stress hormones, also led to an increase of THC. This effect very often is connected to the release of haemocytes from haemopoietic organs. Interestingly, in contrast to our study, this effect usually is observed during few minutes (2–15 min) or/and an hour after stress factors or stress hormones treatment (Adamo, 2010; Mowlds et al., 2008; Strand, 2008). For this reason, this issue needs further investigation.

A statistically significant effect of Tenmo-TRP-7 on phagocytosis was observed only when the peptide was tested directly *in vitro*. However, a smaller immunostatic tendency was observed also 6 and 24 h after injection. This effect was observed only in higher concentrations ( $10^{-5}$  M in case of injection and  $10^{-6}$  M in case of direct application), which may support the over-excitation hypothesis. This hypothesis assumes that high concentration of stress hormone reduces the activity of different immune mechanisms to protect host against autoimmunological injuries, which also can be related to activity of haemocytes (Adamo, 2010; Elenkov and Chrousos, 2006; Schmid-Hempel, 2005). On the other hand, we cannot exclude a possible cytotoxic effect, which partially is confirmed by analysis of DNA integrity. However, a reduction of THC value, which may be also the indicator of cytotoxicity, were not observed.

In vertebrates, SP stimulates for example the adhesion of macrophages and respiratory bursts of natural killer cells (O'Connor et al., 2004). Our results indicate an immunostatic effect of TRPs on insect haemocytes, which is more akin to effects of stress hormones in insects.

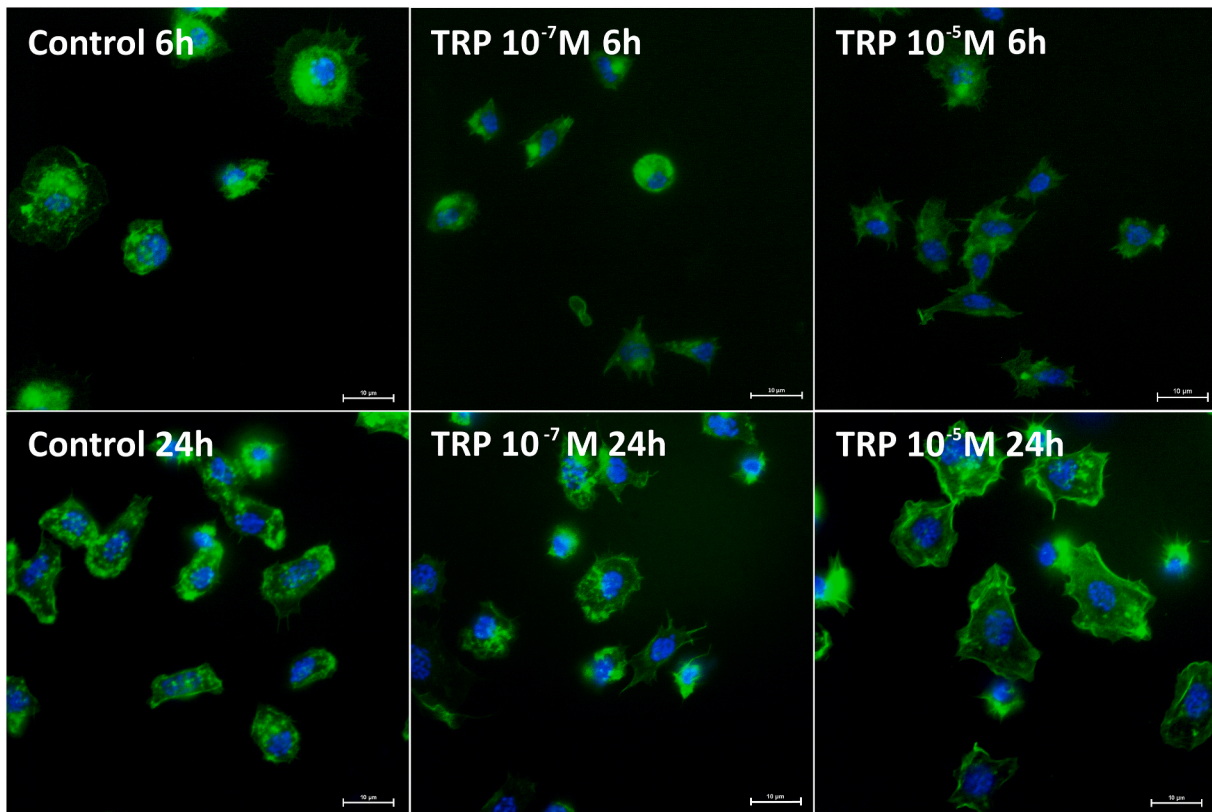


**Fig. 6.** Representative fluorescent photos of *Tenebrio molitor* haemocytes 6 and 24 h after injection of physiological saline (Control) and Tenmo-TRP-7 in concentration  $10^{-7}$  and  $10^{-5}$  M. Green – F-actin cytoskeleton stained with Oregon Green™ 488 Phalloidin; Blue – nucleic acids visualized by DAPI staining; scale bar – 10  $\mu$ m.

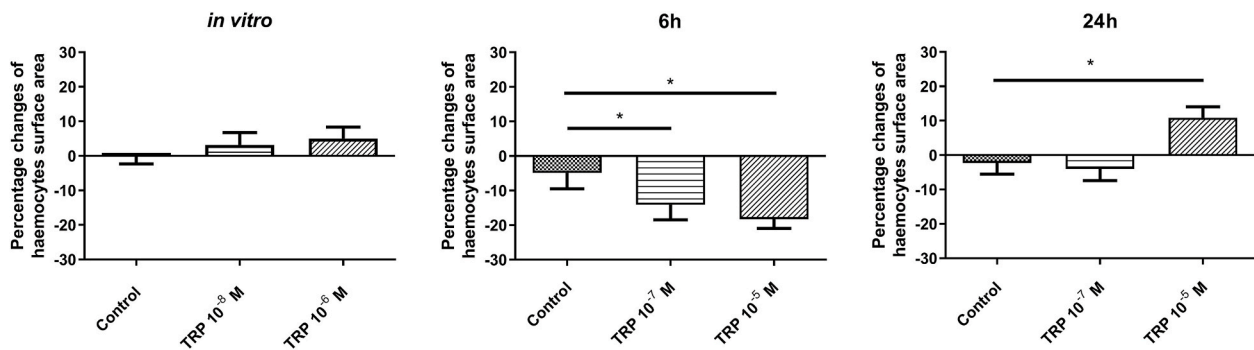


**Fig. 7.** Percentage changes of surface area of *Tenebrio molitor* haemocytes. *in vitro* - haemocytes collected from non-injected individuals, the direct effect was examined by adding Tenmo-TRP-7 in concentrations corresponding to neuropeptide concentrations in the insect body after injection  $10^{-7}$  M and  $10^{-5}$  M dilution (final concentration  $10^{-8}$  M and  $10^{-6}$  M); 6 and 24 h – haemocytes collected 6 or 24 h after application of Tenmo-TRP-7 in concentration  $10^{-7}$  M and  $10^{-5}$  M. The results are expressed as a percentage change compared to control individuals injected physiological saline or non-injected beetles (*in vitro*). Values are means  $\pm$  SEM. \* $p \leq 0.05$  ( $n \geq 7$ ).

The latter would be consistent with the finding that decreased phagocytic ratio was observed in case of high concentration of TRPs which may be characteristic for prolonged stress condition. (Adamo, 2012). Yet, we cannot rule out that TRPs change other haemocyte functions such as respiratory burst or nodulation processes. Also, direct mechanisms of influence of TRP on haemocytes activity is not known.

The results on the influence of Tenmo-TRP-7 on phagocytosis and THC are closely related to haemocyte morphology. For this reason, in the present study haemocyte morphology was studied based on the arrangement of the F-actin cytoskeleton and the cellular surface area, which is an indicator of time of sedimentation and adhesion ability (Urbański et al., 2018). Under all treatments, the F-actin cytoskeleton

was well-developed. The influence of Tenmo-TRP-7 on haemocyte surface area was time- and dose-dependent. After 6 h a decrease of surface area compared to control was noted, but after 24 h at a concentration of  $10^{-5}$  M an increase of surface area was reported. These results suggest that Tenmo-TRP-7 can change haemocyte behaviour in different stages of a stress response. Cells which are characterized by possessing good chemotactic abilities, important for phagocytosis, have a small adhesion ability (Urbański et al., 2018; Valerius et al., 1981). According to these data, it is possible that TRPs change haemocytes behaviour and increase their mobility, which may be crucial at the initial stage of immune response for the PRR process and/or wound healing. On the other hand, significant increases of haemocyte surface area 24 h after application of

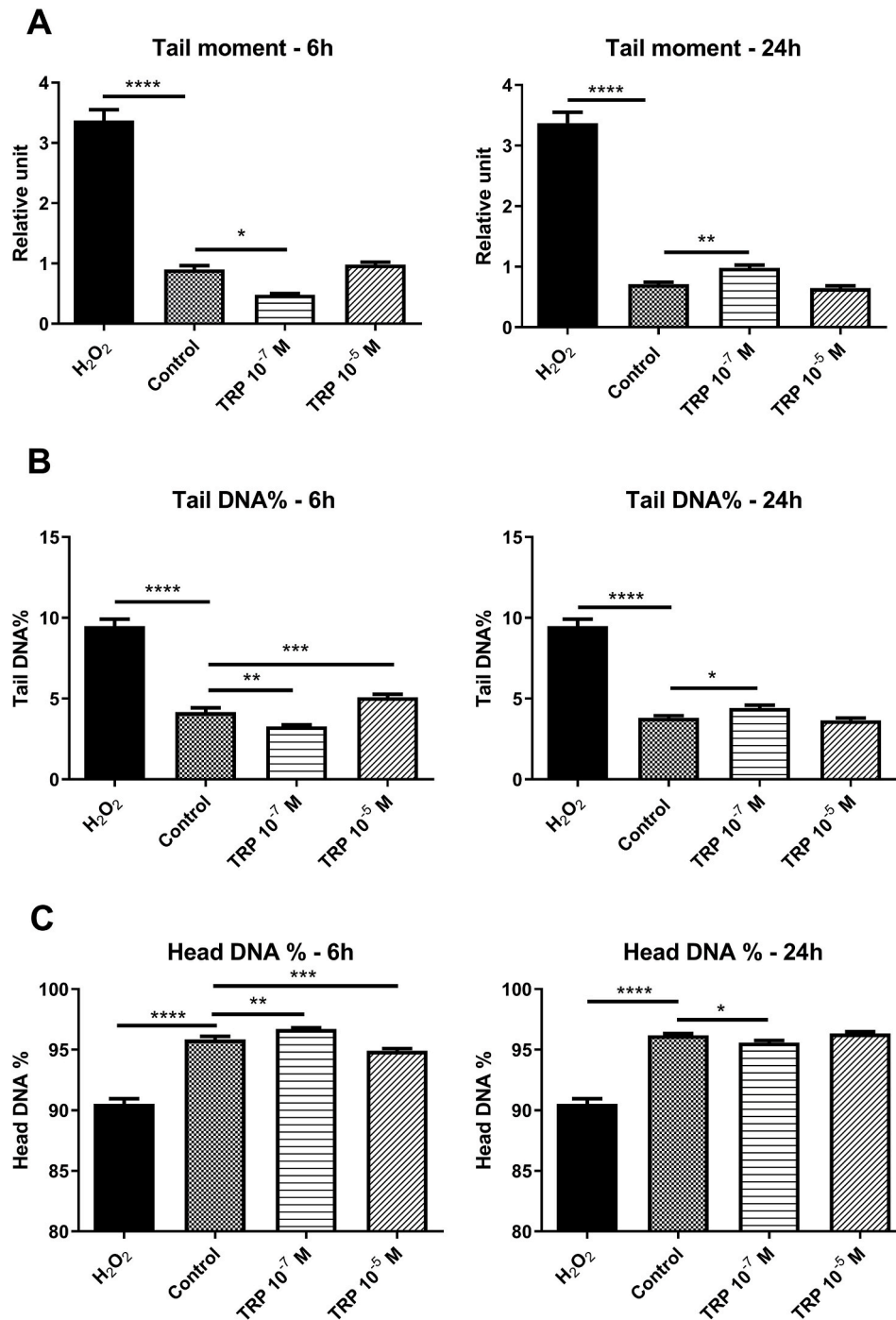


**Fig. 8.** Effects of Tenmo-TRP-7 injection (in concentration  $10^{-7}$  M and  $10^{-5}$ , 6 and 24 h after injection) on DNA damages of *Tenebrio* haemocytes expressed as tail moment (A), tail DNA% (B) and head DNA% (C). H<sub>2</sub>O<sub>2</sub> - positive control, Control – individuals injected with physiological saline. Values are means  $\pm$  SEM; \* $p \leq 0.05$ ; \*\* $p \leq 0.01$ ; \*\*\* $p \leq 0.001$  \*\*\*\*;  $p \leq 0.0001$  ( $n = 5-6$ ). The results of positive control were compared only to Control individuals.

Tenmo-TRP-7 in concentration  $10^{-5}$  M may be important during nodulation process and the later phase of wound healing (Lavine and Strand, 2002).

Because of the possible cytotoxic effect of Tenmo-TRP-7, we studied DNA damage. The effect of Tenmo-TRP-7 was time- and dose-dependent, 6 h after application of Tenmo-TRP-7 ( $10^{-7}$  M) the lowest DNA damage was observed. However, after 24 h the opposite effect was reported. In case of higher concentration, only after 6 h analysis of head DNA% and tail DNA% indicate a cytotoxic effect of TRP. After 24 h this effect could be masked by a release of new haemocytes from the haemopoietic organ. Our results are consistent with the action of SP in vertebrates. For

example, research by Böckmann et al. (2001) and Kang et al. (2001) showed that SP can delay neutrophils and macrophages apoptosis by inhibition of caspase cascade which is very important to regulate the inflammation process. Due to the deep structural homology between SP and TRP, one can speculate that this also occurs in insects.

The insect cellular response also strongly depends on the activity of phenoloxidase (PO) (Cerenius et al., 2008). This enzyme is involved in cuticle melanisation, pathogen recognition and nodule formation (Cerenius et al., 2008). Our results show that injection of Tenmo-TRP-7 increased PO activity, and this effect was especially visible after 6 h after the neuropeptide application. Similar results were observed also in

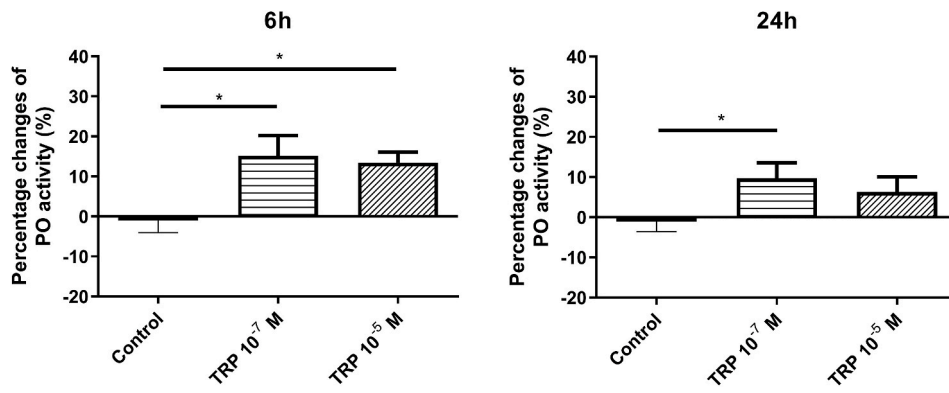


Fig. 9. Phenoloxidase activity in *Tenebrio molitor* haemolymph after injection of Tenmo-TRP-7 in concentration 10<sup>-7</sup> M and 10<sup>-5</sup> M, 6 and 24 h after injection, compared to control individuals injected physiological saline (Control). Values are means ± SEM. \**p* ≤ 0.05 (*n* ≥ 10).

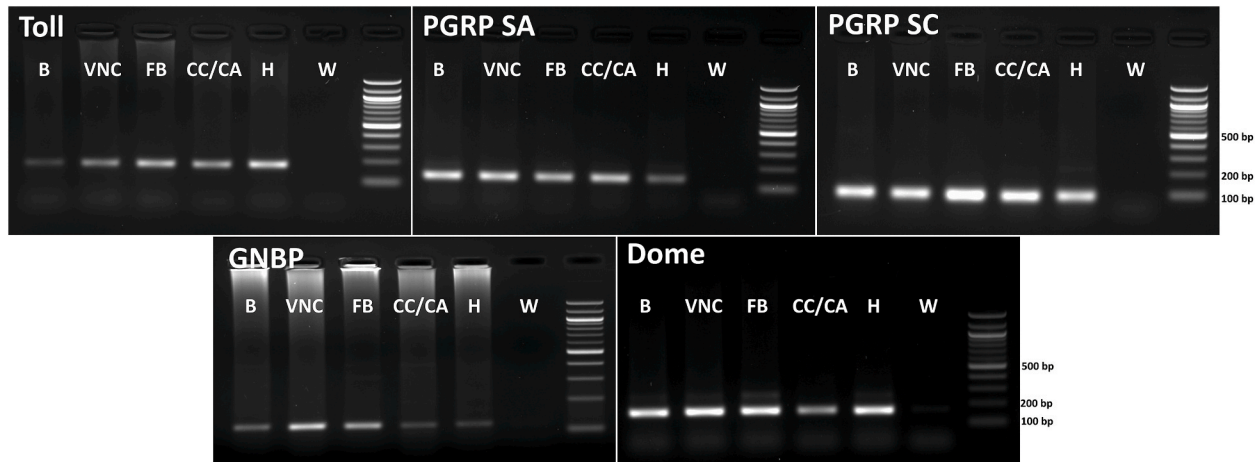


Fig. 10. Expression of genes encoding chosen receptors in different tissues of *Tenebrio molitor*; B – brain; VNC – ventral nerve cord; FB – fat body; CC/CA – retrocerebral complex H – haemocytes; W – water.

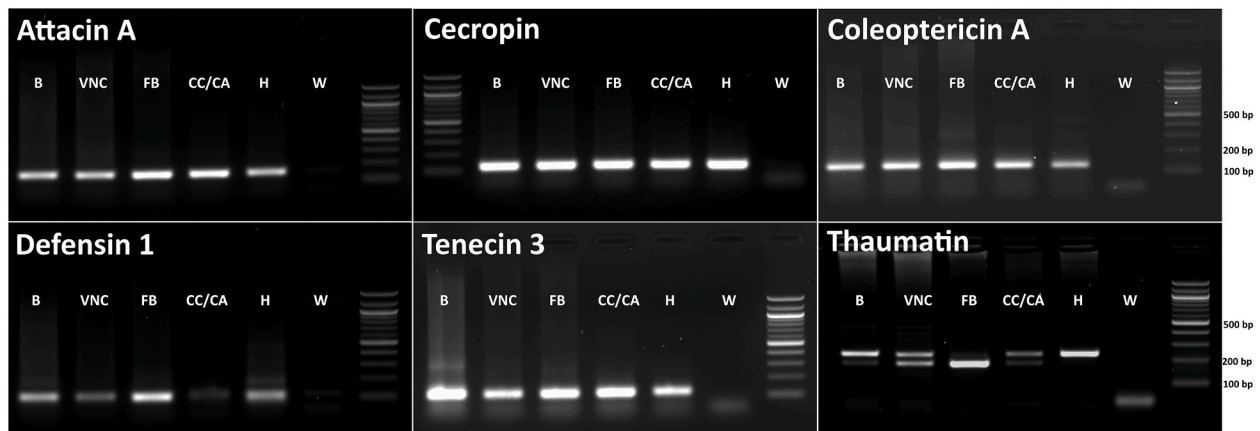


Fig. 11. Tissue distribution of chosen AMPs transcripts in *Tenebrio molitor*; B – brain; VNC – ventral nerve cord; FB – fat body; CC/CA – retrocerebral complex H – haemocytes; W – water.

case of other insect hormones, including stress hormones like AKH or OCT (Baines et al., 1992; Goldsworthy et al., 2003b).

In the light of our results on possible interaction between the insect nervous tissue and the immune system, we also studied the presence of immune-related gene expression in the nervous system of *T. molitor*. The involvement of the nervous system in immune responses has been shown

across the animal kingdom, especially in vertebrates. Moreover, nervous tissues are also involved in the pathogen recognition process, which was confirmed in many species, including humans (Kielian, 2006; Kigerl et al., 2014). Also, bacterial infections and cytokines presence result in increasing concentrations of neuropeptides in human central nervous system (CNS), also SP (Kessler et al., 1993; Suvas, 2017). However, only

very limited data exist in this context in insects. For example, in *Drosophila* neurodegeneration of the brain during prolonged inflammation was described and this correlated with an over-expression of genes encoding PGRPs and AMPs (Kounatidis et al., 2017). Consistent with the results obtained by Kounatidis et al. (2017), we found the expression of genes encoding AMPs and PGRPs in the brain, VNC and retrocerebral complex of *T. molitor*. This also included immune-related pathways, like Toll or JAK/STAT. It should be highlighted that, to the best of our knowledge, this is the first report about strict localization of immune-related genes in different parts of insect nervous tissue, including the retrocerebral complex. Based on these findings, we propose that insect nervous tissue can participate in pathogen recognition processes. Also, there exists a possibility that, similar as in vertebrates, this process indirectly (via cytokines) leads to neuropeptides releasing from neuroendocrine cells, which may regulate insect immune responses against pathogen infection. In particular, it is indicated by the presence of transcripts characteristic for the PRRs and Toll receptors in the retrocerebral complex, that participate in the synthesis of hormones, their storage and release (Urbański and Rosiński, 2018). In addition, the presence of transcripts of genes encoding receptors such as Scavengers, Nimrod or Noduler may also indicate a contribution of nervous cells, including glia, to cellular responses (Husemann et al., 2002; Kurucz et al., 2007; Satyavathi et al., 2016). Verification of these assumptions and analysis of the relationships between expression of immune-related genes and TRP application will be a next step in our research.

In summary, our results may suggest an immunostatic activity of Tenmo-TRP-7 in *T. molitor* in a time- and dose-dependent manner. Also, some of our results, for example PO activity indicate that TRP injection can lead to the stimulation of some of the immune mechanisms. All of these results suggest that the role of TRP, and other stress hormones, during stress response changes over the time of the response. This is consistent with immunotropic, but also immunostatic activities of hormones, including other neuropeptides. For example, AKH speeds-up the nodulation process and PO activity in locusts (Goldsworthy et al., 2003a) but also reduces antimicrobial activity and host resistance to pathogen infection (Goldsworthy et al., 2005). Following the hypothesis proposed by Adamo (2014) about adaptive reconfiguration of the immune system, these differences may be related to rearrangement of immune system functioning during stress response and switching the function of some elements participating in immune processes regulation. A good example is apolipoprotein III which is involved in the pathogen recognition process and also enhances lysozyme activity, but during stress response, is used mainly for lipid transport (Adamo, 2008; Zdybicka-Barabas et al., 2013). Inhibition of certain immune mechanisms activity are compensated by stimulation of other parts of this system, because all biological systems maintain homeostasis (Adamo, 2014). Moreover, in insect several hormonal feedback loops seem to exist and also presence of neuropeptides leads to releasing of other hormones (for example Locmi-TRP leads to the release of AKHs) which contributes to the general response of insects to pathogen infection, including activation of the immune system (Nässel et al., 1995; Urbański and Rosiński, 2018).

#### 4.1. Conclusions

In the manuscript we present an analysis of immunomodulatory action of Tenmo-TRP-7 on activity of chosen cellular and humoral mechanism in *T. molitor*. Obtained results suggest that TRP may influence immune system activity, and observed effects may be time- and dose-dependent. Also, probable presence of TRPR on *T. molitor* haemocytes may indicate the direct effect of tested neuropeptide on the cellular mechanisms. Interestingly, similar to SP, injection of Tenmo-TRP-7 lead to a decrease in the number of DNA damages, which may support our supposition concerning functional homology between TKs and TRPs. Moreover, the evaluation of presence of immune-related genes in the different parts of *T. molitor* nervous tissue may be an interesting starting

point for the analysis on the participation of the insect CNS in the pathogen recognition process and further research about hormonal regulation of insect immune system.

#### Acknowledgement

AU was supported by a scholarship from Polish National Agency for Academic Exchange (NAWA), within the Bekker Programme, 2019 (personal stipend, PPN/BEK/2019/1/00167) and scholarship from the Deutscher Akademischer Austauschdienst (DAAD), within the program for Research Stays for University Academics and Scientists, 2018 (personal stipend, 91696887).

#### Appendix A. Supplementary data

Supplementary data to this article can be found online at <https://doi.org/10.1016/j.dci.2021.104065>.

#### References

- Adamo, S., 2008. Norepinephrine and octopamine: linking stress and immune function across phyla. *Invertebrate Surviv* 5, 12–19.
- Adamo, S., 2010. Why should an immune response activate the stress response? Insights from the insects (the cricket *Gryllus texensis*). *Brain Behav. Immun.* 24, 194–200.
- Adamo, S.A., 2012. The effects of the stress response on immune function in invertebrates: an evolutionary perspective on an ancient connection. *Horm. Behav.* 62, 324–330.
- Adamo, S.A., 2014. The effects of stress hormones on immune function may be vital for the adaptive reconfiguration of the immune system during fight-or-flight behavior. *Integr. Comp. Biol.* 54 (3), 419–426.
- Adamo, S.A., 2017. Stress responses sculpt the insect immune system, optimizing defense in an ever-changing world. *Dev. Comp. Immunol.* 66, 24–32.
- Baines, D., DeSantis, T., Downer, R.G., 1992. Octopamine and 5-hydroxytryptamine enhance the phagocytic and nodule formation activities of cockroach (*Periplaneta americana*) haemocytes. *J. Insect Physiol.* 38, 905–914.
- Bass, C., Katanski, C., Maynard, B., Zurro, I., Mariane, E., Matta, M., Loi, M., Melis, V., Capponi, V., Muroli, P., Setzu, M., Nichols, R., 2014. Conserved residues in RF-NH2 receptor models identify predicted contact sites in ligand–receptor binding. *Peptides* 53, 278–285.
- Blom, N., Sicheritz-Pontén, T., Gupta, R., Gammeltoft, S., Brunak, S., 2004. Prediction of post-translational glycosylation and phosphorylation of proteins from the amino acid sequence. *Proteomics* 4, 1633–1649.
- Böckmann, S., Seep, J., Jonas, L., 2001. Delay of neutrophil apoptosis by the neuropeptide substance P: involvement of caspase cascade. *Peptides* 22, 661–670.
- Cerenius, L., Lee, B.L., Söderhäll, K., 2008. The proPO-system: pros and cons for its role in invertebrate immunity. *Trends Immunol.* 29, 263–271.
- Chowanski, S., Adamski, Z., Lubawy, J., Marciniak, P., Pacholska-Bogalska, J., Slocinska, M., Spochacz, M., Szymczak, M., Urbanski, A., Walkowiak-Nowicka, K., 2017. Insect peptides—perspectives in human diseases treatment. *Curr. Med. Chem.* 24, 3116–3152.
- Czarniewska, E., Mrowczynska, L., Kuczer, M., Rosinski, G., 2012. The pro-apoptotic action of the peptide hormone Neb-colloostatin in insect haemocytes. *J. Exp. Biol.* 215, 4308–4313.
- Diniz, L.C.L., Alves, F.L., Miranda, A., Silva Junior, P.I.d., 2020. Two tachykinin-related peptides with antimicrobial activity isolated from *Triatoma infestans* hemolymph. *Microbiol. Insights* 13, 1178636120933635.
- El-Shazely, B., Urbanski, A., Johnston, P., Rolff, J., 2019. In vivo exposure of insect AMP resistant *Staphylococcus aureus* to an insect immune system. *Insect Biochem. Mol. Biol.* 60–68.
- Elenkov, I.J., Chrousos, G.P., 2006. Stress system—organization, physiology and immunoregulation. *Neuroimmunomodulation* 13, 257–267.
- Goldsworthy, G., Chandrakant, S., Opoku-Ware, K., 2003a. Adipokinetic hormone enhances nodule formation and phenoloxidase activation in adult locusts injected with bacterial lipopolysaccharide. *J. Insect Physiol.* 49, 795–803.
- Goldsworthy, G., Mullen, L., Opoku-Ware, K., Chandrakant, S., 2003b. Interactions between the endocrine and immune systems in locusts. *Physiol. Entomol.* 28, 54–61.
- Goldsworthy, G., Opoku-Ware, K., Mullen, L., 2005. Adipokinetic hormone and the immune responses of locusts to infection. *Ann. N. Y. Acad. Sci.* 1040, 106–113.
- Gyori, B.M., Venkatachalam, G., Thiagarajan, P.S., Hsu, D., Clement, M.V., 2014. OpenComet: an automated tool for comet assay image analysis. *Redox Biol* 2, 457–465.
- Hauser, F., Cazzamali, G., Williamson, M., Park, Y., Li, B., Tanaka, Y., Predel, R., Neupert, S., Schachtner, J., Verleyen, P., 2008. A genome-wide inventory of neurohormone GPCRs in the red flour beetle *Tribolium castaneum*. *Front. Neuroendocrinol.* 29, 142–165.
- Hernández-Martínez, S., Sánchez-Zavaleta, M., Brito, K., Herrera-Ortiz, A., Ons, S., Noriega, F.G., 2017. Allatotropin: a pleiotropic neuropeptide that elicits mosquito immune responses. *PLoS One* 12, e0175759.

- Ho, W.-Z., Lai, J.-P., Zhu, X.-H., Uvaydova, M., Douglas, S.D., 1997. Human monocytes and macrophages express substance P and neurokinin-1 receptor. *J. Immunol.* 159, 5654–5660.
- Husemann, J., Loike, J.D., Anankov, R., Febbraio, M., Silverstein, S.C., 2002. Scavenger receptors in neurobiology and neuropathology: their role on microglia and other cells of the nervous system. *Glia* 40, 195–205.
- Jacobs, C.G., Gallagher, J.D., Evison, S.E., Heckel, D.G., Vilcinskas, A., Vogel, H., 2017. Endogenous egg immune defenses in the yellow mealworm beetle (*Tenebrio molitor*). *Dev. Comp. Immunol.* 70, 1–8.
- Johnston, P.R., Makarova, O., Rolff, J., 2014. Inducible defenses stay up late: temporal patterns of immune gene expression in *Tenebrio molitor*. *G3* 4, 947–955.
- Kang, B.-N., Jeong, K.-S., Park, S.-J., Kim, S.-H., Kim, T.-H., Kim, H.-J., Ryu, S.-Y., 2001. Regulation of apoptosis by somatostatin and substance P in peritoneal macrophages. *Regul. Pept.* 101, 43–49.
- Kessler, J.A., Freidin, M.M., Kalberg, C., Chandross, K.J., 1993. Cytokines regulate substance P expression in sympathetic neurons. *Regul. Pept.* 46, 70–75.
- Kielian, T., 2006. Toll-like receptors in central nervous system glial inflammation and homeostasis. *J. Neurosci. Res.* 83, 711–730.
- Kigerl, K.A., de Rivero Vaccari, J.P., Dietrich, W.D., Popovich, P.G., Keane, R.W., 2014. Pattern recognition receptors and central nervous system repair. *Exp. Neurol.* 258, 5–16.
- Kounatidis, I., Chtarbanova, S., Cao, Y., Hayne, M., Jayanth, D., Ganetzky, B., Ligoxygakis, P., 2017. NF- $\kappa$ B immunity in the brain determines fly lifespan in healthy aging and age-related neurodegeneration. *Cell Rep.* 19, 836–848.
- Kurucz, É., Márkus, R., Zsámboki, J., Folkl-Medzihradzsky, K., Darula, Z., Vilmos, P., Udvardy, A., Krausz, L., Lukacsovich, T., Gateff, E., 2007. Nimrod, a putative phagocytosis receptor with EGF repeats in *Drosophila* plasmatocytes. *Curr. Biol.* 17, 649–654.
- Lavine, M., Strand, M., 2002. Insect hemocytes and their role in immunity. *Insect Biochem. Mol. Biol.* 32, 1295–1309.
- Li, X.-J., Wolfgang, W., Wu, Y.N., North, R.A., Forte, M., 1991. Cloning, heterologous expression and developmental regulation of a *Drosophila* receptor for tachykinin-like peptides. *EMBO J.* 10, 3221.
- Lubawy, J., Daburon, V., Chowański, S., Słocińska, M., Colinet, H., 2019. Thermal stress causes DNA damage and mortality in a tropical insect. *J. Exp. Biol.* 222.
- Marciniak, P., Urbański, A., Kudlewska, M., Szymczak, M., Rosiński, G., 2017. Peptide hormones regulate the physiological functions of reproductive organs in *Tenebrio molitor* males. *Peptides* 98, 35–42.
- Marciniak, P., Urbański, A., Lubawy, J., Szymczak, M., Pacholska-Bogalska, J., Chowański, S., Kuczer, M., Rosiński, G., 2020. Short neuropeptide F signaling regulates functioning of male reproductive system in *Tenebrio molitor* beetle. *J. Comp. Physiol. B* 190, 521–534.
- Mashaghi, A., Marmalidou, A., Tehrani, M., Grace, P.M., Pothoulakis, C., Dana, R., 2016. Neuropeptide substance P and the immune response. *Cell. Mol. Life Sci.* 73, 4249–4264.
- Monaco-Shawver, L., Schwartz, L., Tuluc, F., Guo, C.J., Lai, J.P., Gunnam, S.M., Kilpatrick, L.E., Banerjee, P.P., Douglas, S.D., Orange, J.S., 2011. Substance P inhibits natural killer cell cytotoxicity through the neurokinin-1 receptor. *J. Leukoc. Biol.* 89, 113–125.
- Mowlds, P., Barron, A., Kavanagh, K., 2008. Physical stress primes the immune response of *Galleria mellonella* larvae to infection by *Candida albicans*. *Microb. Infect.* 10, 628–634.
- Nachman, R.J., Moyna, G., Williams, H.J., Zabrocki, J., Zadina, J.E., Coast, G.M., Broeck, J., 1999. Comparison of active conformations of the insect tachykinin/tachykinin and insect Kinin/Tyr-W-MIF-1 Neuropeptide family pairs. *Ann. N. Y. Acad. Sci.* 897, 388–400.
- Nagai-Okatani, C., Nagasawa, H., Nagata, S., 2016. Tachykinin-related peptides share a G protein-coupled receptor with ion transport peptide-like in the silkworm *Bombyx mori*. *PLoS One* 11, e0156501.
- Nässel, D.R., 1999. Tachykinin-related peptides in invertebrates: a review. *Peptides* 20, 141–158.
- Nässel, D.R., Vullings, H.G., Passier, P.C., Lundquist, C.T., Schoofs, L., Diederens, J.H., Van der Horst, D.J., 1999. Several isoforms of locust tachykinins may be involved in cyclic AMP-mediated release of adipokinetic hormones from the locust *Corpora cardiaca*. *Gen. Comp. Endocrinol.* 113, 401–412.
- Nässel, D.R., Passier, P.C., Elekes, K., Dirksen, H., Vullings, H.G., Cantera, R., 1995. Evidence that locust tachykinin I is involved in release of adipokinetic hormone from locust *Corpora cardiaca*. *Regul. Pept.* 57, 297–310.
- Nugent, T., Jones, D.T., 2009. Transmembrane protein topology prediction using support vector machines. *BMC Bioinf.* 10, 159.
- O'Connor, T.M., O'Connell, J., O'Brien, D.I., Goode, T., Bredin, C.P., Shanahan, F., 2004. The role of substance P in inflammatory disease. *J. Cell. Physiol.* 201, 167–180.
- Ren, J., Wen, L., Gao, X., Jin, C., Xue, Y., Yao, X., 2008. CSS-Palm 2.0: an updated software for palmitoylation sites prediction. *Protein Eng. Des. Sel.* 21, 639–644.
- Satyavathi, V.V., Narra, D., Nagaraju, J., 2016. Nodular an immune protein augments infection-induced cell proliferation through cross-talking with p38 MAPK. *Immunobiology* 221, 387–397.
- Schmid-Hempel, P., 2005. Evolutionary ecology of insect immune defenses. *Annu. Rev. Entomol.* 50, 529–551.
- Sorrentino, R.P., Small, C.N., Govind, S., 2002. Quantitative analysis of phenol oxidase activity in insect hemolymph. *Biotechniques* 32, 815–816.
- Strand, M.R., 2008. The insect cellular immune response. *Insect Sci.* 15, 1–14.
- Suvas, S., 2017. Role of substance P neuropeptide in inflammation, wound healing, and tissue homeostasis. *J. Immunol.* 199, 1543–1552.
- Untergasser, A., Cutcutache, I., Koressaar, T., Ye, J., Faircloth, B.C., Remm, M., Rozen, S.G., 2012. Primer3—new capabilities and interfaces. *Nucleic Acids Res.* 40 (15), e115–e115.
- Urbański, A., Adamski, Z., Rosiński, G., 2018. Developmental changes in haemocyte morphology in response to *Staphylococcus aureus* and latex beads in the beetle *Tenebrio molitor* L. *Micron* 104, 8–20.
- Urbański, A., Czarniewska, E., Baraniak, E., Rosiński, G., 2014. Developmental changes in cellular and humoral responses of the burying beetle *Nicrophorus vespilloides* (Coleoptera, Silphidae). *J. Insect Physiol.* 60C, 98–103.
- Urbański, A., Rosiński, G., 2018. Role of neuropeptides in the regulation of the insect immune system—Current knowledge and perspectives. *Curr. Protein Pept. Sci.* 19, 1201–1213.
- Valerius, N.H., Stendahl, O., Hartwig, J.H., Stossel, T.P., 1981. Distribution of actin-binding protein and myosin in polymorphonuclear leukocytes during locomotion and phagocytosis. *Cell* 24, 195–202.
- Van Loy, T., Vandersmissen, H.P., Poels, J., Van Hiel, M.B., Verlinden, H., Broeck, J.V., 2010. Tachykinin-related peptides and their receptors in invertebrates: a current view. *Peptides* 31, 520–524.
- Zdybicka-Barabas, A., Stączek, S., Mak, P., Skrzypiec, K., Mendyk, E., Cytryńska, M., 2013. Synergistic action of *Galleria mellonella* apolipoprotein III and lysozyme against Gram-negative bacteria. *Biochim. Biophys. Acta Biomembr.* 1828, 1449–1456.
- Ziegler, R., Isoe, J., Moore, W., Riehle, M.A., Wells, M.A., 2011. The putative AKH Receptor of the tobacco hornworm, *Manduca sexta*, and its expression. *J. Insect Sci.* 11, 1–20.